

Simulating single-spin dynamics on an IBM five-qubit chip: An approach for undergraduate

Hércules S. Santana,* Francisco D. S. Gomes,[†] and Émerson M. Alves[‡]

*Departamento de Física, Universidade Regional do Cariri,
Av. Leão Sampaio, 107, Triângulo,
63041-145, Juazeiro do Norte, Ceará, Brasil*

Alan C. Santos[§]

*Instituto de Física, Universidade Federal Fluminense,
Av. Gal. Milton Tavares de Souza s/n, Gragoatá,
24210-346 Niterói, Rio de Janeiro, Brazil*

(Dated: June 11, 2019)

Abstract

In this paper we show how the IBM superconducting chips can be a powerful tool for teaching foundations of quantum mechanics for undergraduate students (for graduates as well, in some cases). To this end, we briefly discuss about the main elements of the IBM Quantum Experience platform necessary to understand this paper, i.e., how to implement operations and single-qubit measurements. As the application, we experimentally study the dynamics of single spin systems interacting with static and time-dependent magnetic fields. First, we study the resonant behavior of a single spin coupled to a time-dependent rotating magnetic field. To end, we study the Larmor precession phenomenon. In both cases we show theoretical and real experimental implementation. This article could be useful in introductory courses like quantum mechanics and nuclear magnetic resonance foundations, for example.

I. INTRODUCTION

In traditional courses of quantum mechanics where we introduce the notion of single-spin dynamics, some interesting results are discussed in a purely theoretical way, without any experimental implementation or verification. Obviously, it is due to particular financial limitation in some physical institutes. In particular, the answer to some questions can not be verified and we need the students to believe in what has been said in class. On the other hand, simulating quantum physics is an interesting task we can accomplish in the IBM Team's quantum platform, namely, the IBM Quantum Experience (IBM-QE)¹. From such platform we have access to a five-qubit² in which we can manipulate it from unitary operations (unitary operators) and measurements. This platform has been used to experimentally confirm some theoretical results on quantum information and computation³⁻⁷ as well as to implement high technology quantum protocols like teleportation^{8,9} and among others¹⁰⁻¹³. In this paper we discuss how useful the IBM-QE can be in a physics teaching scenario, where we develop a didactic strategy to deal with the problem of experimentally present the foundations of a single-spin dynamics in presence of a magnetic field, including time-dependent ones.

To this end, we first present the relevant elements that we need to know before starting the simulation of the examples we will present here. We discuss about the unitary operators we will use in our simulations and how we can implement measurement of magnetization in IBM-QE. By the way, we adopt an approach which allow us to introduce how measurement of some physical quantities are performed in a Nuclear Magnetic Resonance (NMR) experimental setup¹⁴. Then, we discuss about the first interesting phenomena of single-spin dynamics, namely *spin resonance* phenomena, associated with a $\frac{1}{2}$ -spin particle in presence of a strong static field along z -direction and a rotating magnetic field. We discuss how the resonance phenomena emerges from a suitable choice of the rotating magnetic field frequency and how it allows us to promote transitions between “spin up” and “spin down” states of the system, even when such rotating field is weakly interacting with the system^{14,15}. To end, we study the Larmor spin precession behavior.

II. THE IBM QUANTUM EXPERIENCE

The five-qubit IBM quantum chip is composed by five superconducting transmon qubits^{16,17} operating at a temperature scale around 5 mK²⁰. In particular, we can perform simulations, and even so experimental realizations, from two different quantum chips, known as the IBM Q 5 Tenerife (ibmqx4) and IBM Q 5 Yorktown (ibmqx2) quantum chips. Particularly, throughout this article we implement the experiments on IBM Q 5 Yorktown quantum chip, due the good decoherence time scale of its qubits¹. In this section we discuss on some important elements of the IBM-QE to be considered in this paper, but more information about IBM-QE quantum chips can be obtained from a number of papers in literature⁸, as well as from the own IBM-QE team beginners guide¹⁸.

A. IBM-QE single-qubit operations

The relevant (to this paper) single-qubit operations implemented on a IBM five-qubit chip are

$$U_1(\lambda) = \begin{bmatrix} 1 & 0 \\ 0 & e^{i\lambda} \end{bmatrix}, U_2(\lambda, \phi) = \begin{bmatrix} \frac{1}{\sqrt{2}} & -\frac{e^{i\lambda}}{\sqrt{2}} \\ \frac{e^{i\phi}}{\sqrt{2}} & \frac{e^{i(\lambda+\phi)}}{\sqrt{2}} \end{bmatrix}, U_3(\lambda, \phi, \theta) = \begin{bmatrix} \cos\left(\frac{\theta}{2}\right) & -e^{i\lambda} \sin\left(\frac{\theta}{2}\right) \\ e^{i\phi} \sin\left(\frac{\theta}{2}\right) & e^{i(\lambda+\phi)} \cos\left(\frac{\theta}{2}\right) \end{bmatrix}, \quad (1)$$

where λ , ϕ and θ are free real parameters which can be adjusted in accordance with gate to be implemented. It is possible to see that the gates $U_1(\lambda)$ and $U_2(\lambda, \phi)$ can be obtained from gate $U_3(\lambda, \phi, \theta)$, but under experimental viewpoint the gates $U_1(\lambda)$ and $U_2(\lambda, \phi)$ can be more efficient than its counterpart obtained from $U_3(\lambda, \phi, \theta)$. In fact, each gate needs a time to be implemented, where $U_1(\lambda)$ does not take time to be implemented (more precisely, the gate time duration can be neglected), $U_2(\lambda, \phi)$ is a gate with duration of 1 unit of gate time and $U_3(\lambda, \phi, \theta)$ is implemented with duration of 2 units of gate time. Therefore, it is most convenient to use the gates $U_1(\lambda)$ and $U_2(\lambda, \phi)$ whenever possible.

B. Measuring physical quantities

In particular, the IBM-QE allows us to implement measurements in computational basis $|0\rangle \equiv |\uparrow\rangle$ and $|1\rangle \equiv |\downarrow\rangle$, i.e., given a quantum state $|\psi\rangle = a|\uparrow\rangle + b|\downarrow\rangle$, the output of a measurement provides the values of $|a|^2$ and $|b|^2$. Thus, the physical quantities which we can measure in IBM-QE are constrained to that one which can be obtained from parameters $|a|^2$ and $|b|^2$. For example, if we want to measure the expected value of the spin along z direction, we have

$$\mathcal{M}_z = \langle \psi | S_z | \psi \rangle = \frac{\hbar}{2} (|a|^2 - |b|^2) . \quad (2)$$

Thus, it is possible to compute \mathcal{M}_z . In addition, if we want to compute the expected value of spin along x direction, we need to compute $\mathcal{M}_x = \langle \psi | S_x | \psi \rangle$. It can be done if we define the operator

$$H = \frac{1}{\sqrt{2}} \begin{bmatrix} 1 & 1 \\ 1 & -1 \end{bmatrix} , \quad (3)$$

where one uses the relation $S_x = HS_zH$ to write

$$\mathcal{M}_x = \langle \psi | HS_zH | \psi \rangle = \langle \psi_x | S_z | \psi_x \rangle , \quad (4)$$

with $|\psi_x\rangle = H|\psi\rangle$. In quantum computation, the operator H is a Hadamard gate and it can be implemented on IBM-QE. In conclusion, it means we can measure \mathcal{M}_x if implemented a Hadamard gate on the state $|\psi\rangle$ before measure the state in computational basis. In the same way, a measurement of $\mathcal{M}_y = \langle \psi | S_y | \psi \rangle$ can be done if we implement the operation

$$R_x(\pi) = \frac{1}{\sqrt{2}} \begin{bmatrix} 1 & i \\ i & 1 \end{bmatrix} , \quad (5)$$

which represents a rotation of π around axis x . In fact, we can show that $S_y = R_z(\pi)S_zR_x^\dagger(\pi)$, so that

$$\mathcal{M}_y = \langle \psi | S_y | \psi \rangle = \langle \psi | R_z(\pi)S_zR_x^\dagger(\pi) | \psi \rangle = \langle \psi_y | S_z | \psi_y \rangle , \quad (6)$$

with $|\psi_y\rangle = R_x^\dagger(\pi)|\psi\rangle$. Thus, we can measure any spin magnetization around the directions x , y and z . In addition, we can perform measurement of any physical quantity \mathcal{O} which can be written as $\mathcal{O} = R_{\hat{r}}(\phi)S_zR_{\hat{r}}^\dagger(\phi)$, where $R_{\hat{r}}(\phi)$ denotes a rotation of ϕ around direction \hat{r} , from equation

$$\mathcal{O} = \langle \psi | \mathcal{O} | \psi \rangle = \langle \psi | R_{\hat{r}}(\phi)S_zR_{\hat{r}}^\dagger(\phi) | \psi \rangle . \quad (7)$$

III. SINGLE-SPIN DYNAMICS ON IBM QUANTUM EXPERIENCE

The spin is a inner degree of freedom of the electron which can be manipulated with external magnetic fields. In particular, for a $\frac{1}{2}$ -spin particle we have two distinct states $|\uparrow\rangle$ and $|\downarrow\rangle$. These two states satisfy the eigenvalue equation

$$S_z|\uparrow\rangle = \frac{\hbar}{2}|\uparrow\rangle \quad \text{and} \quad S_z|\downarrow\rangle = -\frac{\hbar}{2}|\downarrow\rangle, \quad (8)$$

in which \hbar is the reduced Planck's constant and $S_n = (\hbar/2)\sigma_n$, where σ_n ($n = \{x, y, z\}$) denotes the Pauli matrices for a two-level system given by (with $i = \sqrt{-1}$)

$$\sigma_x = \begin{bmatrix} 0 & 1 \\ 1 & 0 \end{bmatrix}, \quad \sigma_y = \begin{bmatrix} 0 & -i \\ i & 0 \end{bmatrix} \quad \text{and} \quad \sigma_z = \begin{bmatrix} 1 & 0 \\ 0 & -1 \end{bmatrix}, \quad (9)$$

so that the matrix form for the basis $|\uparrow\rangle$ and $|\downarrow\rangle$ reads as $|\uparrow\rangle = [1 \ 0]^t$ and $|\downarrow\rangle = [0 \ 1]^t$, with subscript “t” denoting transpose of a matrix.

A. Simulating Nuclear Magnetic Resonance phenomenon

Let us consider the coupling dynamics of a single $\frac{1}{2}$ -spin with a rotating magnetic field $\vec{B}(t)$ given by

$$\vec{B}(t) = \vec{B}_0 + \vec{B}_{\text{rf}}(t), \quad (10)$$

where $\vec{B}_0 = B_0\hat{z}$ is strong around Z -direction and $\vec{B}_{\text{rf}}(t)$ is a time-dependent transverse magnetic fields, given by

$$\vec{B}_{\text{rf}}(t) = B_{\text{rf}}[\cos(\omega t)\hat{x} + \sin(\omega t)\hat{y}], \quad (11)$$

where ω is the rotating frequency of the transverse magnetic field, also known as Radio-Frequency (rf) field. Therefore, the coupling energy of the system with the field yields the Hamiltonian

$$H(t) = -\vec{\mu} \cdot \vec{B}(t) = \frac{\hbar\omega_0}{2}\sigma_z + \frac{\hbar\omega_{\text{rf}}}{2}[\cos(\omega t)\sigma_x + \sin(\omega t)\sigma_y], \quad (12)$$

where ω_0 is the Larmor frequency and ω_{rf} is the coupling of the spin with rf-field. The solution of the Schrödinger equation for the system is known and given by¹⁵

$$|\psi(t)\rangle = \exp\left[-\frac{i\omega}{\hbar}t\sigma_z\right] \exp\left[-\frac{i}{\hbar}\tilde{H}t\right] |\psi(0)\rangle, \quad (13)$$

where

$$\tilde{H} = \hbar \frac{\omega_0 - \omega}{2} \sigma_z + \hbar \frac{\omega_{RF}}{2} \sigma_x . \quad (14)$$

In matrix form, we write each evolution operator as

$$U_0(t) = \exp \left[-\frac{i}{\hbar} \frac{\omega}{2} t \sigma_z \right] = e^{-\frac{i\omega t}{2}} \begin{bmatrix} 1 & 0 \\ 0 & e^{-i\omega t} \end{bmatrix} , \quad (15)$$

$$U_{xz}(t) = \exp \left[-\frac{i}{\hbar} \tilde{H} t \right] = \begin{bmatrix} \cos \left(\frac{\Omega t}{2} \right) + i \frac{\Delta}{\Omega} \sin \left(\frac{\Omega t}{2} \right) & i \frac{\omega_{rf}}{\Omega} \sin \left(\frac{\Omega t}{2} \right) \\ i \frac{\omega_{rf}}{\Omega} \sin \left(\frac{\Omega t}{2} \right) & \cos \left(\frac{\Omega t}{2} \right) - i \frac{\Delta}{\Omega} \sin \left(\frac{\Omega t}{2} \right) \end{bmatrix} , \quad (16)$$

where $\Delta = \omega_0 - \omega$ is a detuning between the rf-field and the Larmor frequencies, and $\Omega^2 = \Delta^2 + \omega_{rf}^2$ is the effective Rabi frequency, which takes into account effects due the detuning¹⁹. It is worth to mention that the factored term $e^{-\frac{i\omega t}{2}}$ in $U_0(t)$ represents a global phase and will be neglected from now on. In particular, here we will simulate the resonance phenomena, in which a small rf-field ($|\omega_{rf}| \ll |\omega_0|$) can be used to flip the spin state when the rf-field oscillation frequency is close to ω $|\Delta| \rightarrow 0$. Under this configuration, the operator $U_{xz}(t)$ becomes

$$U_{xz}^{\text{ress}}(t) = \begin{bmatrix} \cos \left(\frac{\omega_{rf} t}{2} \right) & i \sin \left(\frac{\omega_{rf} t}{2} \right) \\ i \sin \left(\frac{\omega_{rf} t}{2} \right) & \cos \left(\frac{\omega_{rf} t}{2} \right) \end{bmatrix} , \quad (17)$$

and the system will evolve as

$$|\psi^{\text{ress}}(t)\rangle = U_0(t) U_{xz}^{\text{ress}}(t) |\psi(0)\rangle . \quad (18)$$

In case where the initial state is given by $|\psi(0)\rangle = |\uparrow\rangle$, by computing time-dependence of the Z -spin component we get

$$\mathcal{M}_z(t) = \langle \psi(t) | S_z | \psi(t) \rangle = \frac{\hbar}{2} \cos(\omega_{rf} t) . \quad (19)$$

Notice that the parameter ω does not develop any role in above quantity. We choose this particular state because the standard input state in IBM quantum chip is the computational state $|0\rangle$, namely the spin-up state $|\uparrow\rangle$.

To simulate the spin dynamics of the Eq. (18) we need to map the evolution operators $U_0(t)$ and $U_{xz}^{\text{ress}}(t)$ into available parameters in IBM-QE. We mean, from Eqs. (1) we need to identify each the operator $U_0(t)$ with $U_1(\lambda_1)$ and the operator $\mathcal{U}_{\text{ress}}(t)$ with $U_3(\lambda, \phi, \theta)$ for

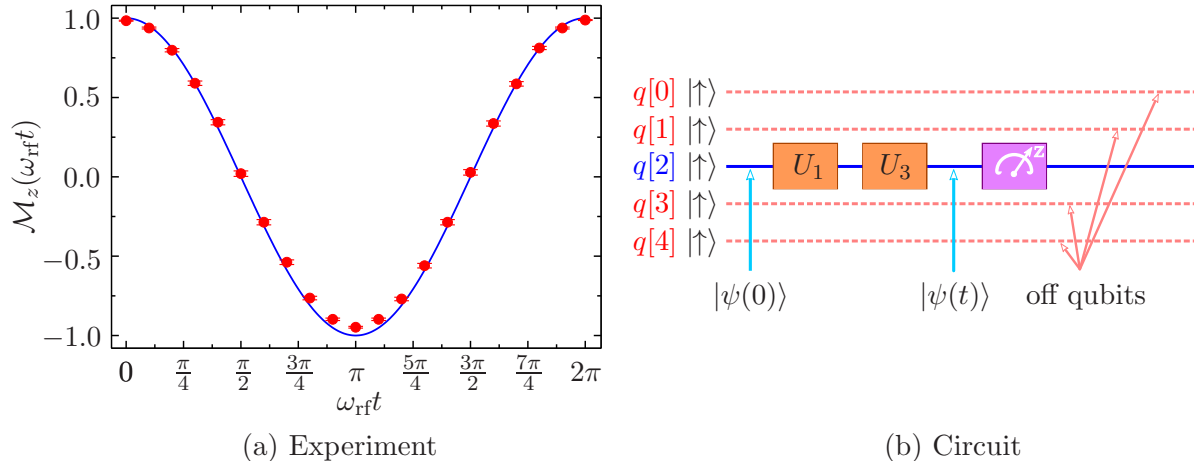


Figure 1: (1a) Theoretical (line) and experimental data (dots) of the single spin magnetization at resonance. In our experiment we set $N = N_{\max} = 8192$ shots. (1b) Circuit implemented on IBM Q 5 Yorktown chip (ibmqx2), where we highlight the qubit used in experiment (continuum blue line) while the rest of the qubit were taken off during the experiment (dashed light red line). The magenta box represents a measurement in computational basis.

a particular choice of the parameters λ , ϕ and θ . A first point to be highlighted is that λ , ϕ and θ are dimensionless parameters, so we need to link dimensionless parameters of $U_0(t)$ and $U_{xz}^{\text{ress}}(t)$ to those ones in operators $U_1(\lambda_1)$ and $U_3(\lambda, \phi, \theta)$. In our case, it is possible to see that $U_1(-\omega t) = U_0(t)$ and $U_3(\frac{3\pi}{2}, \frac{\pi}{2}, \frac{\omega_{\text{rf}} t}{2}) = \mathcal{U}_{\text{ress}}(t)$. In conclusion, $\mathcal{U}_{\text{ress}}(t)$ would be simulated through the sequence

$$\mathcal{U}_{\text{ress}}^{\text{sim}}(t) = U_1(-\omega t)U_3\left(\frac{3\pi}{2}, \frac{\pi}{2}, \frac{\omega_{\text{rf}} t}{2}\right), \quad (20)$$

whose the circuit is shown in Fig. 1. In Fig. 1a we present the theoretical and experimental data of the resonant spin dynamics. To this end, we encode our spin to be driven by Hamiltonian in Eq. (12) on qubit $q[2]$ as shown in Fig. 1b. As provided by IBM team before we start the experiment, the experimental chip configuration are present in table I. After implement the unitary operations (which simulate the dynamics), we measure the Z -magnetization component in order to see some spin flip in the system (as expected in resonance situation). As expected, within an experimental error, the theoretical and experimental are in agreement. The error bar is computed from relation²¹ $\Delta p = \pi\sqrt{p_0(1-p_0)/N}$, where N is the number of experimental shoots and $p_0 = |\langle 0|\psi\rangle|^2$.

Table I: Physical parameters obtained from last calibration before the experimental implementation shown in Fig.1. For this experiment, the calibration date is 2019-05-24 08:04:12 AM.

Parameters	$q[0]$	$q[1]$	$q[2]$	$q[3]$	$q[4]$
Frequency (GHz)	5.29	5.24	5.03	5.3	5.08
T1 (μ s)	53.40	62.10	65.50	60.90	49.50
T2 (μ s)	42.20	54.40	57.20	28.90	59.90
Gate error (10^{-3})	3.35	1.55	4.64	3.44	5.84
Readout error (10^{-2})	4.80	24.20	1.70	1.70	32.00

B. Spin precession

Now, as a second application, let us discuss the experimental simulation of the Lamor precession. By considering the system at initial state

$$|\psi_0\rangle = \cos\left(\frac{\theta}{2}\right)|\uparrow\rangle + \sin\left(\frac{\theta}{2}\right)|\downarrow\rangle, \quad (21)$$

where $\theta \in [0, \pi]$. If the system is driven by a time-independent magnetic field along z -direction, i.e., $\vec{B}_0 = B_0\hat{z}$, the associated Hamiltonian is read as

$$H_0 = \frac{\hbar\omega_0}{2}\sigma_z, \quad (22)$$

whose the evolved system will be given by (up to a global phase)

$$|\psi(t)\rangle = \tilde{U}_0(t)|\psi_0\rangle = \cos\left(\frac{\theta}{2}\right)|\uparrow\rangle + e^{i\omega t}\sin\left(\frac{\theta}{2}\right)|\downarrow\rangle, \quad (23)$$

where $\tilde{U}_0(t) = e^{-\frac{i}{\hbar}H_0t} = \text{diag}[1 \quad e^{i\omega t}]$ is the evolution operator, a bit different from $U_0(t)$ given in Eq. (15). Now, by computing the behavior of the physical quantities defined in Eqs. (2), (4) and (6), we get

$$\mathcal{M}_z = \frac{\hbar}{2}\cos(\theta), \quad \mathcal{M}_x(t) = \frac{\hbar}{2}\sin(\theta)\cos(\omega_0t), \quad \mathcal{M}_y(t) = \frac{\hbar}{2}\sin(\theta)\sin(\omega_0t). \quad (24)$$

Now, in order to see the precession behavior, if we define the magnetization vector $\vec{\mathcal{M}}_{xy}$ in xy -plane as

$$\vec{\mathcal{M}}_{xy} = \mathcal{M}_x\hat{x} + \mathcal{M}_y\hat{y}, \quad (25)$$

we conclude that

$$\vec{\mathcal{M}}_{xy} = \sin(\theta)[\cos(\omega_0t)\hat{x} + \sin(\omega_0t)\hat{y}], \quad (26)$$

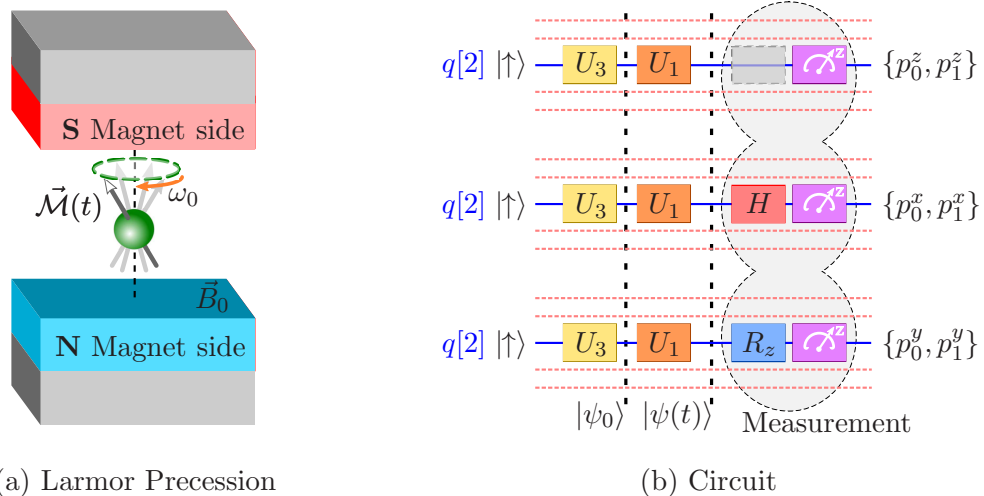


Figure 2: (2a) Sketch of a single-spin inside a static magnetic field along Z -direction, where the precession behavior is highlighted. (2b) Circuit used for each dynamics and measurement implemented on IBM Q 5 Yorktown chip (ibmqx2), where we highlight the qubit used in experiment (continuum blue line) while the rest of the qubit are taken off during the experiment (dashed light red line). The magenta box represents a measurement in computational basis and provide us the probabilities $\{p_0^{x,y,z}, p_1^{x,y,z}\}$.

which represents a vector with norm $|\sin(\theta)|$ rotating in xy -plane around z -axis. Therefore, when we define the magnetization vector $\vec{\mathcal{M}} = \mathcal{M}_z \hat{x} + \vec{\mathcal{M}}_{xy}$ we get

$$\vec{\mathcal{M}}(t) = \cos(\theta) \hat{x} + \sin(\theta) [\cos(\omega_0 t) \hat{x} + \sin(\omega_0 t) \hat{y}] , \quad (27)$$

since $\mathcal{M}_z = \cos(\theta)$. The geometrical representation of $\vec{\mathcal{M}}(t)$ is shown in Fig. 2a. For this reason, we call such dynamics *Larmor spin precession*.

To simulate such a dynamics, we need to prepare the initial input state $|\psi_0\rangle$, then implement the evolution as provided by evolution operator $\tilde{U}_0(t)$ and finally to measure the magnetization along directions x , y and z . Thus, the circuit which simulates the Larmor spin precession is presented in Fig. 2 and we can build it following three steps:

- (1) The initial state: As mentioned, the IBM-QE has a natural input state given by $|0\rangle = |\uparrow\rangle$, so any algorithm input state should be achieved from it. In particular, the initial state $|\psi_0\rangle$ can be obtained from $|\uparrow\rangle$ through the unitary operation

$$U_{\text{inp}} = \begin{bmatrix} \cos\left(\frac{\theta}{2}\right) & -\sin\left(\frac{\theta}{2}\right) \\ \sin\left(\frac{\theta}{2}\right) & \cos\left(\frac{\theta}{2}\right) \end{bmatrix} . \quad (28)$$

Table II: Physical parameters obtained from last calibration before the experimental implementation shown in Fig.3. For this experiment, the last calibration date is 2019-05-29 08:07:25 AM.

Parameters	$q[0]$	$q[1]$	$q[2]$	$q[3]$	$q[4]$
Frequency (GHz)	5.29	5.24	5.03	5.3	5.08
T1 (μ s)	21.90	51.10	70.10	60.30	50.40
T2 (μ s)	26.50	42.10	62.20	27.10	51.20
Gate error (10^{-3})	9.28	1.46	4.21	3.95	3.44
Readout error (10^{-2})	9.50	26.10	1.60	3.70	37.90

The above unitary operator is obtained from gate $U_3(\lambda, \phi, \theta)$ in Eq. (1) if we set $\lambda = 0$ $\phi = 0$. Thus, we have $U_{\text{inp}} = U_3(0, 0, \theta)$.

- (2) The evolution: As previously discussed, the evolution as provided by operator $\tilde{U}_0(t)$ can be achieved through the $U_1(\lambda)$ gate (up to a global phase) whenever we set $\lambda = \omega_0 t$.
- (3) The measurement: The last circuit step is the measurement. To measure the z -magnetization we don't need to implement rotations, since the natural measurement basis performed by IBM-EQ is the computational basis ("spin-up-spin-down" basis in our case). The magnetization measurement along x and y direction is obtained as discussed in Sec. II B, so we need to implement a Hadamard (H) gate and $R_z = R_z(\pi)$ gate to measure in x and y basis, respectively.

The experiment of the precession spin was implemented with same qubit as in previous experiment, but with new physical parameters as shown in Table II. In experiment we have two dimensionless parameters to be adjusted, namely the parameter θ associated with initial state and the quantity $\omega_0 t$ due the time-dependence of the operator $\tilde{U}_0(t)$. Thus, we choose two values of θ and we experimentally study the behavior of the physical quantities defined in Eq. (24) as function of $\omega_0 t$. Since we need to start the protocol with same state for each measurement, we set the same parameter θ in gate U_3 for each circuit of the Fig. 2b, while we vary the parameter λ of the gate U_1 used to encode the dimensionless value of $\omega_0 t$. Given a same initial for all experiments, each circuits in figures provides us the probabilities values $p_0^{x,y,z}$ and $p_1^{x,y,z}$, then we obtain a set of experimental values of the quantities $\mathcal{M}_{x,y,z}^{\text{exp}}(\omega_0 t)$

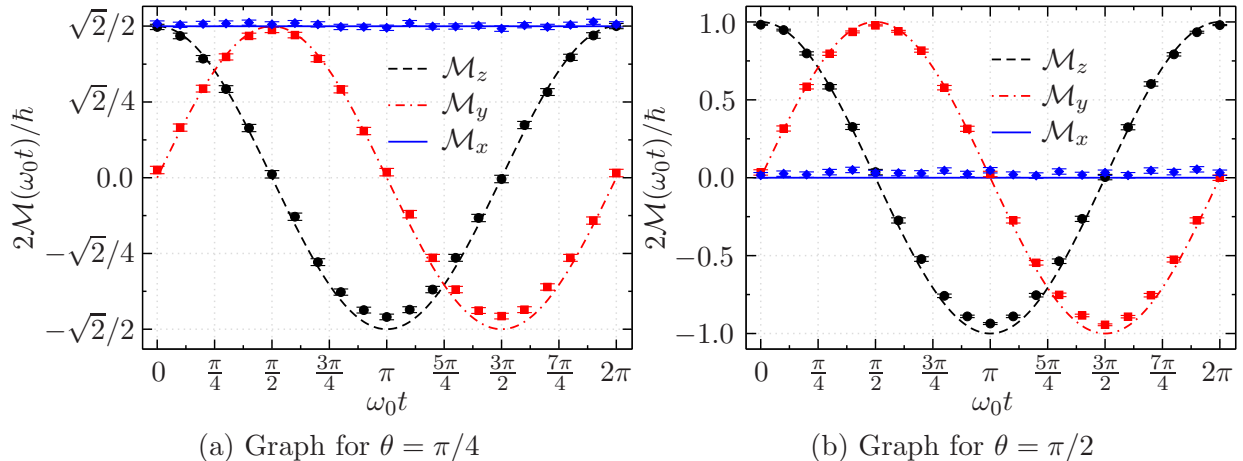


Figure 3: Magnetization \mathcal{M} (in multiple of $\hbar/2$) along the direction x (dashed black curves), y (dashed red dot curves) and z (continuum blue curves) as function of $\omega_0 t$ for the choices (3a) $\theta = \pi/4$ and (3b) $\theta = \pi/2$. In our experiment we set $N = N_{\max} = 8192$ shots and we implement the circuit on IBM Q 5 Yorktown chip (ibmqx2). Points denote the experimental data obtained from IBM-QE platform.

from equation

$$\mathcal{M}_{x,y,z}^{\text{exp}}(\omega_0 t) = \frac{\hbar}{2} [p_0^{x,y,z}(\omega_0 t) - p_1^{x,y,z}(\omega_0 t)] . \quad (29)$$

Therefore, it allows us to compare the experimental result with theoretical values given in Eq. (24) and the results are shown in Fig. 3. Again, we compute the error bar for each circuit from relation²² $\Delta p^{x,y,z} = \pi \sqrt{p_0^{x,y,z}(1 - p_0^{x,y,z})/N}$. Thus, we can see the good agreement between theoretical predictions and experimental data.

IV. CONCLUSION

Here we present a didactic proposal which can be used to present a more consistent study on quantum single-spin dynamics, where we discuss about a possibility of dealing with some experimental limitation due limited financial support of some institutes of physics around the world. To this end, we encourage the usage of the IBM-QE platform as a resource for teaching quantum mechanics from a experimental approach, in completeness with the theoretical one. Here we present the required elements (quantum gates and measurement) to study single-spin dynamics from IBM-QE systems. As a demonstration of how useful

the IBM-QE platform can be, we discuss about two particular and interesting dynamics of single-spin system. As a first example, we can discuss about resonance phenomena in systems composed of nuclear spins, which high applicability in nuclear magnetic resonance based quantum technologies. To end, we study the Larmor precession phenomena. Both applications could be experimentally verified. It is worth to highlight that both experiments were implemented in a relatively short time, for our case, in average, it took between 3 and 10 minutes for getting the experimental data file for each execution (each point of the graph).

Acknowledgments

ACS acknowledges financial support from the Brazilian agencies Conselho Nacional de Desenvolvimento Científico e Tecnológico (CNPq), Brazilian National Institute of Science and Technology for Quantum Information (INCT-IQ) and the Coordenação de Aperfeiçoamento de Pessoal de Nível Superior (CAPES) (Finance Code 001).

* Electronic address: hercules-santana@hotmail.com

† Electronic address: coltan1804@gmail.com

‡ Electronic address: emerson.amn@gmail.com

§ Electronic address: ac'santos@id.uff.br

¹ “Ibm quantum experience”, <https://quantumexperience.ng.bluemix.net/qx/editor>.

² B. Schumacher, “Quantum coding”, *Phys. Rev. A* **51**, 2738–2747 (1995).

³ M. Berta, S. Wehner, and M. M. Wilde, “Entropic uncertainty and measurement reversibility”, *New J. Phys.* **18**, 073004 (2016).

⁴ D. García-Martín and G. Sierra, “Five experimental tests on the 5-qubit ibm quantum computer”, *Journal of Applied Mathematics and Physics* **6**, 1460 (2018).

⁵ R. P. Rundle, P. W. Mills, T. Tilma, J. H. Samson, and M. J. Everitt, “Simple procedure for phase-space measurement and entanglement validation”, *Phys. Rev. A* **96**, 022117 (2017).

⁶ G. W. Dueck, A. Pathak, M. Mazder Rahman, A. Shukla, and A. Banerjee, “Optimization of Circuits for IBM’s five-qubit Quantum Computers”, arXiv e-prints p. arXiv:1810.00129 (2018).

- ⁷ K. Das and A. Sadhu, “Constant Time Quantum search Algorithm Over A Datasets: An Experimental Study Using IBM Q Experience”, arXiv e-prints p. arXiv:1810.03390 (2018).
- ⁸ A. C. Santos, “The ibm quantum computer and the ibm quantum experience”, *Rev. Bras. Ensino Fís.* **39**, e1301 (2017).
- ⁹ S. Fedortchenko, “A quantum teleportation experiment for undergraduate students”, arXiv e-prints p. arXiv:1607.02398 (2016).
- ¹⁰ N. N. Hegade, A. Das, S. Seth, and P. K. Panigrahi, “Investigation of quantum pigeonhole effect in IBM quantum computer”, arXiv e-prints p. arXiv:1904.12187 (2019).
- ¹¹ S. Mahanti, S. Das, B. K. Behera, and P. K. Panigrahi, “Quantum Robots Can Fly; Play Games: An IBM Quantum Experience”, arXiv e-prints p. arXiv:1905.10968 (2019).
- ¹² S. I. Doronin, E. B. Fel’dman, and A. I. Zenchuk, “Solving systems of linear algebraic equations via unitary transformations on quantum processor of IBM Quantum Experience”, arXiv e-prints p. arXiv:1905.07138 (2019).
- ¹³ S. J. Devitt, “Performing quantum computing experiments in the cloud”, *Phys. Rev. A* **94**, 032329 (2016).
- ¹⁴ I. Oliveira, R. Sarthour Jr, T. Bonagamba, E. Azevedo, and J. C. Freitas, *NMR quantum information processing* (Elsevier, Oxford, UK, 2011).
- ¹⁵ M. A. Nielsen and I. L. Chuang, *Quantum Computation and Quantum Information: 10th Anniversary Edition* (Cambridge University Press, New York, NY, USA, 2011), 10th ed.
- ¹⁶ J. Koch, T. M. Yu, J. Gambetta, A. A. Houck, D. I. Schuster, J. Majer, A. Blais, M. H. Devoret, S. M. Girvin, and R. J. Schoelkopf, “Charge-insensitive qubit design derived from the cooper pair box”, *Phys. Rev. A* **76**, 042319 (2007).
- ¹⁷ J. A. Schreier, A. A. Houck, J. Koch, D. I. Schuster, B. R. Johnson, J. M. Chow, J. M. Gambetta, J. Majer, L. Frunzio, M. H. Devoret, S. M. Girvin, and R. J. Schoelkopf, “Suppressing charge noise decoherence in superconducting charge qubits”, *Phys. Rev. B* **77**, 180502 (2008).
- ¹⁸ “Guide for ibm quantum experience”, <https://quantumexperience.ng.bluemix.net/qx/tutorial>.
- ¹⁹ C.-K. Hu, J.-M. Cui, A. C. Santos, Y.-F. Huang, M. S. Sarandy, C.-F. Li, and G.-C. Guo, “Experimental implementation of generalized transitionless quantum driving”, *Opt. Lett.* **43**, 3136–3139 (2018).
- ²⁰ See more details here <https://www.research.ibm.com/ibm-q/learn/what-is-quantum-computing/>

²¹ See <https://quantumexperience.ng.bluemix.net/proxy/tutorial/> for more details on experimental error and decoherence effects

²² See <https://quantumexperience.ng.bluemix.net/proxy/tutorial/> for more details on experimental error and decoherence effects